Macroscopic Stability:
I. “Ideal” stability

F.L. Waelbroeck

Institute for Fusion Studies, The University of Texas at Austin

International Center for Theoretical Physics
25 August 2014

★IFS

Outline

IFS

Outline

In Tokamaks, Macroscopic instabilities can be catastrophic

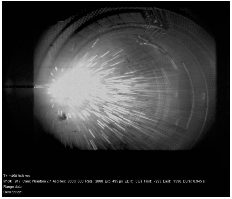

Runaway electrons striking Tore-Supra surface, creating carbon dust shower.

- Macroscopic instabilities that do not saturate result in plasma contact with the wall.
- Due to the toroidal current flowing in tokamak plasmas, this generates large $\mathbf{J} \times \mathbf{B}$ forces acting on the vacuum vessel.
- The inductive fields created during the current quench creates beams of runaway electrons.
- Clearly, macroscopic instabilities must be controlled.

State space and Equilibrium

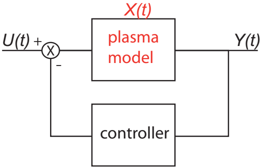

$\dot{X}(t) = f(X(t), U(t), t);$
$Y(t) = g(X(t), U(t), t).$

- Plasmas have infinite degrees of freedom but finite energy, so the state vector X is denumerably infinite-dimensional (think Fourier coefficients). To represent X on a computer it must be *truncated*.
- Think of plasma as a system close to a quiescent, equilibrium state $X_0 = X_0(U)$:

$$\dot{X} = F(X_0, U, t) = 0$$

- We are concerned in this and subsequent talks with formulating and solving the equation for $X(t)$.

Linear analysis of dynamics

- Small motions away from the equilibrium state, $X = X_0 + x$ can be described by Taylor expansion of the rate F:

$$\dot{x} = \mathbf{M}x + O(x^2),$$

where **M** is the Jacobian operator (matrix):

$$\mathbf{M} = \partial F(X, U, t)/\partial X|_{X=X_0} .$$

- Plasma models are usually *non-normal* ($\mathbf{M}^*\mathbf{M} \neq \mathbf{M}\mathbf{M}^*$): MHD is an important exception where $\mathbf{M}^* = \mathbf{M}$.
- For normal operators the eigenvalue decomposition leads to the solution:

$$X(t) = X_0 + \sum e^{i\omega_j t} |u_j\rangle\langle u_j|.$$

Outline

1. Macroscopic Stability of Fusion Plasma
   - Stability
   - Nonlinear evolution
   - Current singularities in bifurcated equilibria
2. Resolving the singular currents: resistive MHD
   - A framework for nonlinear resistive evolution
   - Current diffusion and the rate of reconnection
   - Non-equilibrium effects in magnetic reconnection

Nonlinear evolution of ideal MHD instabilities

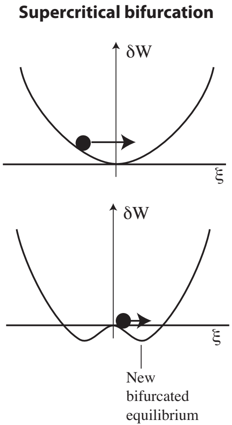

- In practice, the system evolves slowly through a sequence of quasi-equilibria.
- As the system transitions from stability to instability, it evolves smoothly into the nearby stable bifurcated equilibrium.
- Examples include the long lived mode, the edge harmonic oscillation, and possibly the “snake” oscillation.

Stable bifurcations are preceded by long precursors

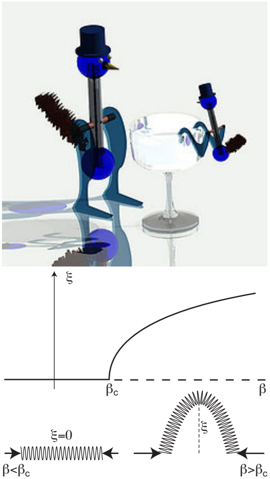

- Typical times scales for sawtooth crash, ELM, disruption $\sim 100\mu s \gg \tau_A \sim 1\mu s$.
- In the drinking bird toy, evaporation draws fluid up the tube, creating an inverted pendulum
- The evaporation rate $\ll \gamma$, so the dip is preceded by a precursor oscillation.
- MHD instabilities, in particular sawtooth crashes and edge localized modes (ELM), often occur with little precursor activity

Subcritical bifurcations do not explain fast onset

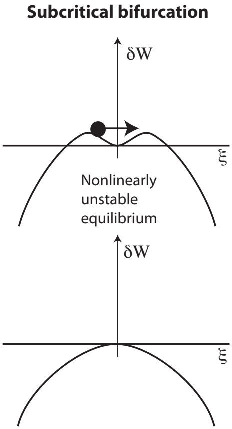

- In principle, a subcritical bifurcation can occur but practical examples are hard to find.
- Clearly, such states are difficult to realize experimentally.
- Within the framework of the MHD model, it is thus difficult to understand the onset of Alfvénic instabilities.
- To understand macro-stability, we must look at the bifurcated equilibria.

Outline

Current singularities are generic in MHD equilibria

- There are two types of singularities in the current-density:
  1. Arising from the flux-conservation property during quasi-static evolution
  2. Arising from Pfirsch-Schlüter currents (providing for the neutralization of diamagnetic currents)
- The relaxation of either of these currents leads to the formation of magnetic islands that degrade plasma confinement.

The resonant bifurcation of a cylindrical equilibrium exhibits a current singularity

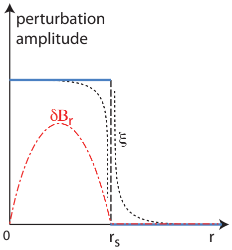

- The equation governing the $m = 1$ harmonic of the plasma displacement is

$$\frac{d}{dr}\left(r^3 k_\parallel^2 \frac{d\xi}{dr}\right) - \epsilon^2 g(r)\xi(r) = 0$$

- Lowest-order solution is “top hat”
- The solution exhibits a singularity described by $J_z \propto \delta(r - r_s) + \delta W/(r - r_s)$.
- Also holds nonlinearly (Rosenbluth ’73).

Asymmetric 3D equilibria exhibit current singularities

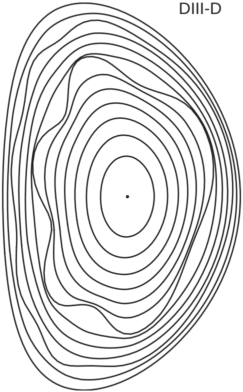

P. Garabedian, PNAS 06

- Force balance, $\mathbf{J}\times\mathbf{B} = \nabla p$, determines $\mathbf{J}_\perp$.
- Charge conservation determines $\mathbf{J}_\|$:

$$\mathbf{B}\cdot\nabla(J_\|/B) = -\nabla\cdot\mathbf{J}_\perp.$$

- Expressing the solution as a Fourier series yields

$$\left[\frac{J_\|}{B}\right]_{mn} = \frac{\mu_0 p'}{\langle B^2\rangle}\sum_{m,n}\frac{\mathcal{G}_{mn}(q)}{q-\frac{m}{n}} + \hat{J}_{mn}\,\delta(q-\frac{m}{n}),$$

Asymmetric 3D equilibria exhibit current singularities

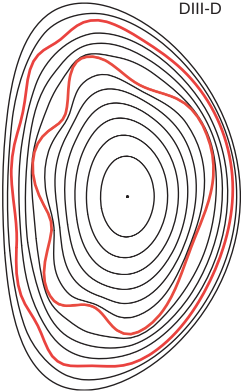

P. Garabedian, PNAS 06

- Force balance, $\mathbf{J} \times \mathbf{B} = \nabla p$, determines $\mathbf{J}_\perp$.
- Charge conservation determines $\mathbf{J}_\|$:

$$\mathbf{B} \cdot \nabla(J_\| / B) = -\nabla \cdot \mathbf{J}_\perp .$$

- Expressing the solution as a Fourier series yields

$$\left[\frac{J_\|}{B}\right]_{mn} = \frac{\mu_0 p'}{\langle B^2 \rangle} \sum_{m,n} \frac{\mathcal{G}_{mn}(q)}{q - \frac{m}{n}} + \hat{J}_{mn}\, \delta(q - \frac{m}{n}),$$

Asymmetric 3D equilibria exhibit current singularities

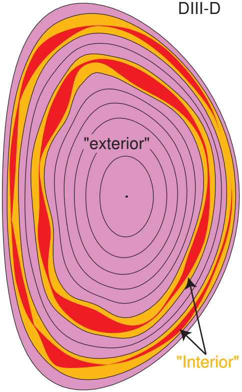

P. Garabedian, PNAS 06

- Force balance, $\mathbf{J} \times \mathbf{B} = \nabla p$, determines $\mathbf{J}_\perp$.
- Charge conservation determines $\mathbf{J}_\parallel$:

$$\mathbf{B} \cdot \nabla(J_\parallel / B) = -\nabla \cdot \mathbf{J}_\perp .$$

- Expressing the solution as a Fourier series yields

$$\left[\frac{J_\parallel}{B}\right]_{mn} = \frac{\mu_0 p'}{\langle B^2 \rangle} \sum_{m,n} \frac{\mathcal{G}_{mn}(q)}{q - \frac{m}{n}} + \hat{J}_{mn}\, \delta(q - \frac{m}{n}),$$

- Calculations divide naturally into an exterior problem and an interior problem

Resistivity and magnetic reconnection

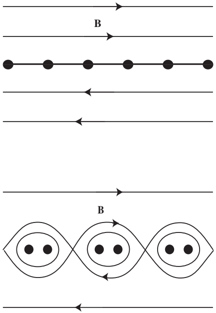

- A current sheet can be thought of as an infinite array of parallel current elements.
- Parallel currents attract so that such an array is unstable to a coagulation or filamentation instability, forming “magnetic islands”:
- This instability is forbidden by the frozen-in law but enabled by resistivity.

Outline

Island evolution is analogous to that of a tokamak

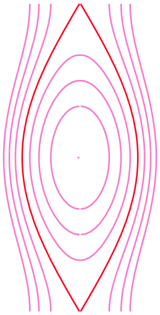

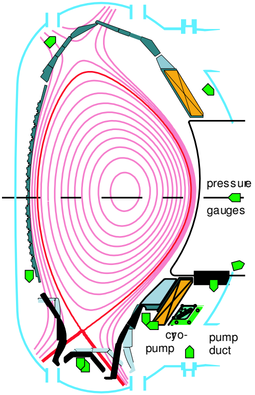

Magnetic island vs. double-null discharge

- Predicting the evolution of magnetic islands is similar to predicting the evolution of a discharge.
- the problem divides into coupled equilibrium and transport equations.

Equilibrium and transport

1. **Transport:** evolution of the profiles given the geometry. This involves solving equations of the type

$$\frac{\partial T(\psi, t)}{\partial t} = \frac{d}{d\psi}\left(\langle\kappa\rangle \frac{dT}{d\psi}\right).$$

2. **Equilibrium:** calculate $\psi(R, Z)$ given the pressure and current profiles. In axisymmetric plasma, this is specified by the Grad-Shafranov Equation:

$$R^2\nabla(R^{-2}\nabla\psi) = -4\pi R^2 \frac{dP}{d\psi} - I\frac{dI}{d\psi}.$$

In a tokamak, the role of the external currents (coils) are often specified through the shape of the last closed flux surface.

For an island, the external currents are specified by Δ'

- Solution of the linear MHD equations outside the island determine

$$\Delta' = \frac{\tilde{\psi}'(0^+) - \tilde{\psi}'(0^-)}{\tilde{\psi}(0)} = \frac{1}{\tilde{\psi}(0)} \int dx\, \tilde{J} \sim \frac{\tilde{B}_y}{\tilde{E}} \sim Y.$$

- Δ' can be thought of as the admittance of the plasma for the shear-Alfvén wave.
- Δ' can also be shown to be proportional to the free energy available for reconnection (Furth et al. 1973).
- Near marginal stability $\Delta' \sim 1/\delta W$, where δW is the ideal MHD energy.

BGK-like solutions for magnetic island equilibria

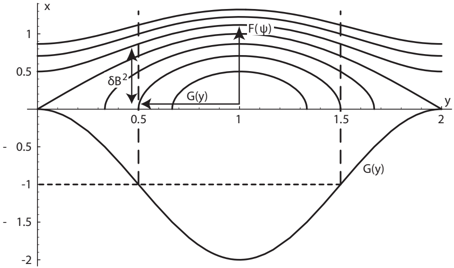

- The equilibrium Eq. is $\mathbf{B}\cdot\nabla J_{\|} = 0$.
- The solution is

$$J_{\|} \simeq \frac{\partial^2\psi}{\partial x^2} = J(\psi) = \frac{dF}{d\psi}.$$

- Integrating once yields

$$B_y = \sqrt{2(F(\psi) - G(y))}.$$

- Integrating again yields

$$x(\psi, y) = x_t(y) \pm \int_{\psi_t}^{\psi} \frac{d\psi}{B_y}.$$

Outline

As concerns transport, there are two types of islands.

- Magnetic islands can be divided into slowly growing and rapidly growing islands depending on how their growth rate compares to the inverse skin time for the island.
    - The skin time is $\tau = W^2/\eta$ where W is the island half-width.
    - The growth rate is $\gamma = \eta J/\psi = \eta\Delta'/W$.

1. **Rutherford regime:** for $\gamma\tau = W\Delta' \ll 1$ The island grows slowly and the profiles are at all time equilibrated. This is the constant-$\tilde{\psi}$ regime first studied by Rutherford (1973).
2. **Sweet-Parker regime:** For $\gamma\tau = W\Delta' \gg 1$ the island grows faster than the current can diffuse, resulting in current singularities and fast reconnection.

The Rutherford regime: $W\Delta' \ll 1$

- For $W\Delta' \ll 1$, $\tilde{J}_z = \nabla^2\tilde{\psi} \ll J_{z0}$ so

$$\psi = \psi_0(x) + \tilde{\psi}(t)\cos y.$$

- The island geometry is entirely determined in terms of its half-width, $W = 2\sqrt{\tilde{\psi}/B_y'}$.
- The growth is determined by Ohm's law

$$\langle\frac{\partial\psi}{\partial t}\rangle = \eta I(\psi) \quad \Longrightarrow \quad \dot{W} = 1.22\eta\Delta'/\mu_0.$$

The Sweet-Parker regime: $W\Delta' \gg 1$

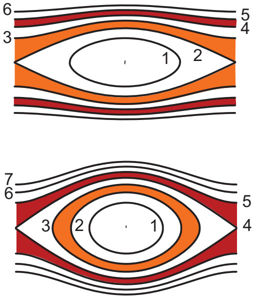

- If the island grows much faster than the skin time W^2/η, the flux is frozen in and helicity is conserved *for all pairs of flux tubes* (B. Kadomtsev 1975):

$$\frac{d\Phi}{d\psi} = \oint_{3-4} \frac{dy}{B_y} = \oint_{3'-4'} \frac{dy}{B_y}.$$

- On the separatrix, the flux-tube volume goes to infinity!

X-point splits into 2 Y-points joined by a current ribbon

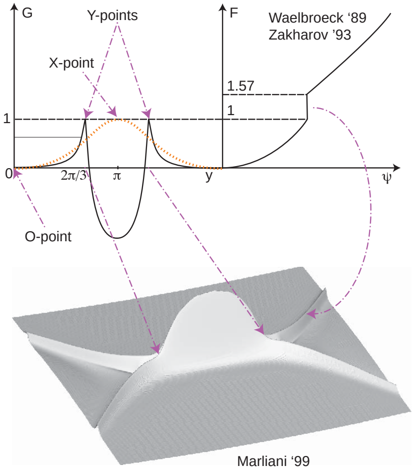

- The helicity conservation constraint for our equilibrium is

$$\frac{1}{x} = \frac{1}{\sqrt{\psi}} = \oint \frac{dy}{\sqrt{F(\psi) - G(y)}}$$

- The only way to satisfy this constraint is to allow the X-point to flatten into a ribbon joining two Y-points.

Current ribbons sustain rapid reconnection

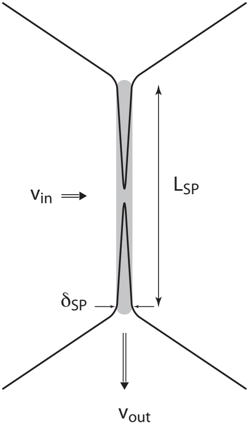

- Energy conservation implies $v_{\text{out}} = V_A$.
- Mass conservation requires

$$v_{\text{in}} L_{SP} = v_{\text{out}} \delta_{SP} = V_A \delta_{SP}$$

- Diffusion across the ribbon implies

$$v_{\text{in}} = V_A L_{SP} / \delta_{SP} S$$

where $S = \eta / V_A L_{SP}$.

- This leads to the Sweet-Parker rate:

$$v_{\text{in}} = S^{-1/2} v_A.$$

Transition from Rutherford to SP and ribbon formation

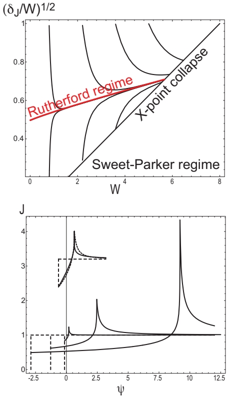

- For chosen profiles, the island width W and current width δ_J specify a family of equilibria.
- The equilibrium equation shows that $J(\psi_s)$ diverges when its *relative width* $\delta_J < \hat{W}/4$.
- Ohm's law at the O-point and separatrix determines the evolution of W and δ_J.
- The evolution equations show that δ_J grows too slowly to avoid the singularity.
- The X-point collapses for $W\Delta' \simeq 25$.

Transition from Rutherford to SP and ribbon formation

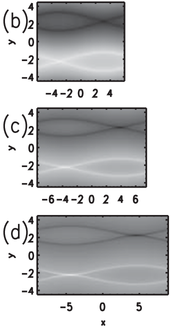

Jemella '04

- For chosen profiles, the island width W and current width δ_J specify a family of equilibria.
- The equilibrium equation shows that $J(\psi_s)$ diverges when its *relative width* $\delta_J < \hat{W}/4$.
- Ohm's law at the O-point and separatrix determines the evolution of W and δ_J.
- The evolution equations show that δ_J grows too slowly to avoid the singularity.
- The X-point collapses for $W\Delta' \simeq 25$.

Numerical results are in good agreement with theory

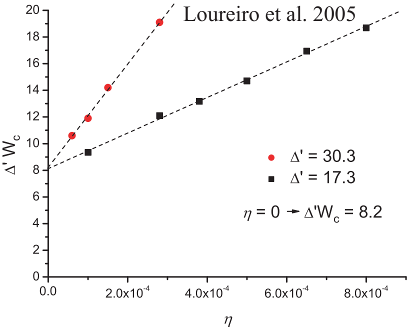

- Simulations show that the critical width depends on the resistivity as well as the profile of the unperturbed current.
- In the limit of vanishing resistivity, the critical width is inversely proportional to Δ' as predicted by analytic theory.

Outline

★IFS

For large Lundquist number, the equilibrium theory fails

- The width of the Sweet-Parker layer scales as $\delta_{SP}/L_{SP} \sim S^{-1/2}$.
- As this width decreases, two things can happen:
  1. The ribbon becomes unstable to secondary instabilities, in particular tearing modes. This is known as the plasmoid reconnection regime.
  2. The ribbon becomes narrower than the Larmor radius, causing polarization effects to become important. This is generally referred to as the Hall reconnection regime.
- Both of the above processes invalidate the equilibrium assumption and make analysis much harder

Tearing mode stability of the SP ribbons and plasmoid reconnection

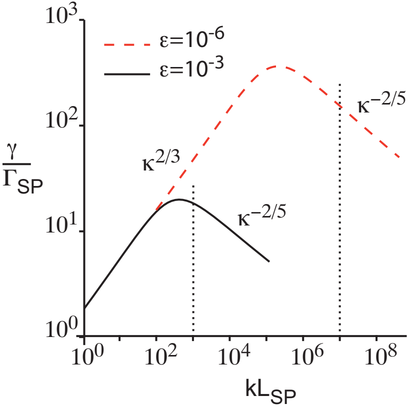

- Simulations show that for $S > 10^4$ the SP ribbon becomes unstable to tearing modes.
- The peak plasmoid growth rate $\gamma = S^{1/4}\Gamma_{SP}$ is reached for $kL_{SP} \sim S^{3/8}$.
- This results in a reconnection rate of $\sim 1\%$, independent of S.

The polarization current accelerates reconnection when the Larmor radius exceeds the layer width

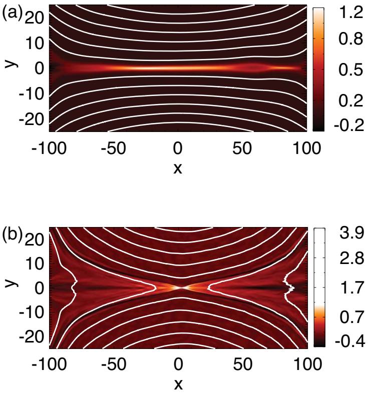

- Simulations show that the ion acceleration near the separatrix gives rise to density holes (recall $\nabla \cdot \mathbf{J}_{\mathrm{pol}} \neq 0$)
- The pressure gradient along the separatrix restores the X-point geometry, enabling faster outflow
- This results in a reconnection rate of $\sim$ 10%, independent of *S*.

Summary

- Ideal MHD predicts slow evolution between saturated equilibria with singular currents on rational surfaces.
- Resistivity gives rise to growing magnetic islands even below the ideal stability threshold.
- There are several regimes of growth depending on the strength of the drive (Δ'), the value of the resistivity, and the Hall parameter:
  1. The Rutherford regime
  2. The Sweet-Parker regime
  3. The plasmoid regime
  4. The Hall-MHD regime